LS-154
9/28/90

The Linac Injector For The ANL 7 GeV Advanced Photon Source

A. Nassiri, W. Wesolowski, and G. Mavrogenes
Argonne National Laboratory

Submitted to the 1990 LINAC Conferece
Albuquerque, New Mexico

THE LINAC INJECTOR FOR THE ANL 7 GeV ADVANCED PHOTON SOURCE*

A. Nassiri, W. Wesolowski, and G. Mavrogenes
Argonne National Laboratory
9700 South Cass Avenue
Argonne, IL 60439 USA

Abstract

The Argonne Advanced Photon Source (APS) linac system consists of a 200 MeV electron linac, a positron converter, and a 450 MeV positron linac. Design parameters and computer simulations of the two linac systems are presented.

Introduction

The Argonne Advanced Photon Source is a 7 GeV synchrotron X-Ray facility. The APS machine parameters have been described.[1] Here, we will focus on the design of the linac systems. We present the results of beam dynamics calculation and computer simulations of the two linac systems.

Electron Linac

General Description

The electron linac components are shown in Figure 1. An electron gun produces pulses of 30 nsec at a 60 Hz repetition rate with a nominal energy of 110 keV and a current of 2.5 A. Each 30 nsec macropulse traverses a standing wave single-gap, pre-buncher operating at 2856 MHz and is broken into approximately 86 micropulses via velocity modulation. After a 22 cm drift space, the micropulse of electrons has been longitudinally compressed to 60°. Further longitudinal compression to 12° is achieved by passing through a constant impedance β = 0.75 travelling waveguide main buncher consisting of six cavities. The reference particle energy at exit of the buncher is about 1.4 MeV. The bunched beam is then accepted and accelerated through five constant gradient travelling waveguides, each approximately 3 m long, to their final energy of more than 200 MeV.

Dynamics of Bunching

The dynamics of bunching have been described before by Slater.[2] In a gap-and-drift buncher, a beam of electrons passes through a single-gap cavity excited by a sinusoidal electric field. For uniform electron velocity, the higher order harmonic effects can be neglected. In the low space charge limit,[3] the change in energy of each electron as it traverses the gap is given as

$$\Delta\gamma(\theta) = -\alpha\, \xi_{gap} \sin\theta_o \qquad (1)$$

$$\theta_o = -\omega t$$

$$\alpha = \frac{eE\lambda}{m_o c^2} = \text{normalized electric field}$$

$$\xi_{gap} = \frac{\Delta z_{gap}}{\lambda} = \text{normalized length of gap}$$

Electrons which reach the gap when $\omega t<0$ are decelerated while electrons which arrive at the gap when $\omega t>0$ will gain energy. As the electrons traverse the drift space, they bunch around the electrons which crossed the gap at $\theta=0$. As the electrons travel the drift space, θ will change as

$$\frac{\Delta\theta(z)}{\Delta\xi} = \frac{2\pi z}{\lambda}\left(\frac{1}{\beta_o} - \frac{1}{\beta}\right) \qquad (2)$$

where β_o is the initial normalized velocity of the electrons.

Integration of the above equation gives θ as a function of ξ along the drift space. Figure 2 illustrates the bunching properties of the gap-and-drift prebuncher. Particles traversing the gap at θ_o=-90 have the highest energy, while particles crossing the gap at +90 have the lowest. At ξ=2.0, electrons are bunched into about 60° of phase.

In the travelling waveguide buncher, assuming a uniform electron velocity, the longitudinal component of the field is written as

$$E_z = E \sin\omega(t-z/v_o) \qquad (3)$$

The equation of motion of an electron in this field is given by:

$$dp/dt = eE \sin\omega(t-z/v_o) \qquad (4)$$

*Work supported by the U.S. Department of Energy, Office of Basic Sciences, under Contract W-31-109-ENG-38.

In a reference frame, moving with velocity v_o of the travelling wave, the displacement z' with respect to the moving frame is $z'=z-vt$.

In this frame the Hamiltonian[2] is given by:

$$H = \sqrt{m_o^2 c^4 + p^2 c^2} - pv_o - eE \frac{v_o}{\omega} \cos \frac{\omega z'}{v_o} \qquad (5)$$

and the equations of motion are derived from the Hamiltonian

$$\frac{dp}{dt} = -\frac{\partial H}{\partial z'}, \quad \frac{dz'}{dt} = \frac{\partial H}{\partial p} \qquad (6)$$

Since the Hamiltonian is not an explicit function of time, it is a constant. Figure 3 shows the phase space plot. The bounded electrons follow a closed orbit about the point $\theta=0$, $p=p_o$. Electrons going slower than the wave lose energy until they fall behind the phase null. They then gain energy until they are synchronous with the wave and they continue to gain energy until they pass the phase null ($\theta=0$). Then they lose energy until they are slower than the synchronous velocity and the cycle repeats.

PARMELA Simulations

PARMELA has been used to design, study, and simulate the beam dynamics in the electron linac. About 65% of the particles can be bunched within approximately 12°. The energy spread at the end of the buncher is approximately 1 MeV. Velocity modulation and longitudinal space charge are the main factors contributing to the energy spread in the bunching system. The electrons next traverse five accelerating sections.

Figure 4 shows the results of beam simulations at the positron target. The reference particle has an energy of over 200 MeV with a current of approximately 1.7 A. A beam spot size of 3 mm and emmitance of $\epsilon \leq 1.2$ mm-mrad can be obtained at the target. It should be mentioned that PARMELA does not take into account the effect of beam loading. However, we have introduced a phase shift of about 15° at the beginning of the second waveguide to simulate the effects of beam loading. The overall energy spread is about ± 8%. This result is in agreement with beam loading calculations using TRANSPORT.

Beam Transport Focusing System

PARMELA and TRANSPORT have been used to design the focusing system for the electron linac. Simulations indicate that a set of three quadrupole triplets are adequate to provide focusing and transport properties.

Positron Production

Following the DESY design, the positrons are produced in a water-cooled, tungsten retractable target of thickness equal to two radiation lengths (7 mm). A double-layered pulsed solenoid located immediately after the target defines the solid-angle acceptance of the positrons. A field strength of 1.5 T is necessary. The accepted positron emittance is $\epsilon=330$ mm-mrad (220 mrad x 1.5 mm) in each transverse plane when a beam size of 1.5 mm radius is used.

Positron Linac

Beam Focusing System

The positrons emerging from the pulsed solenoid are further focused by a solenoidal field of 0.4 T which encompasses the first two positron accelerating structures. The subsequent focusing system consists of a FODO array. COMFORT has been used for beam simulations. Figure 5 shows the beam envelope.

PARMELA Simulation

PARMELA has been adapted[4] to simulate the capture of the positrons from the target through the end of the positron accelerator. Results indicate that one could transport the positrons with a small phase spread, therefore the requirement of a 1% energy spread at 450 MeV can be met. See Figure 6. The normalized emittance of positrons at 450 MeV is 6.6 mm-mrad in each transverse plane.

Acknowledgement

The authors wish to thank R. Miller of SLAC, L. Young of LANL, and C. Kim of LBL for helpful discussions.

References

1. "7 GeV Advanced Photon Source Conceptual Design Report" ANL-87-15, April, 1987.

2. J. C. Slater, "Review of Modern Physics 20, p 473 (1948).

3. Mary Beth James, "Production of High Intensity Electron Buncher for the SLAC Linear Collier," PhD Thesis, SLAC Report 319 (1987).

4. A. Nassiri, Unpublished Report.

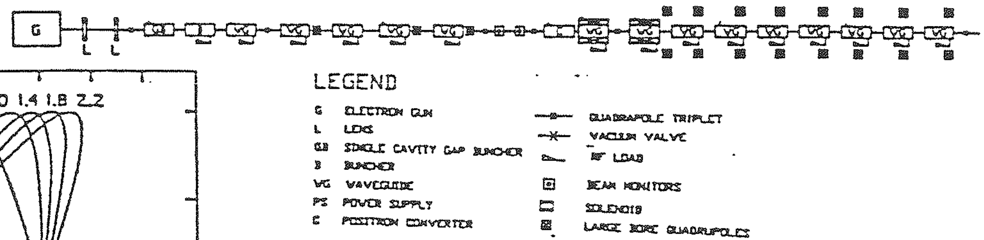

Figure 1 Linac Components

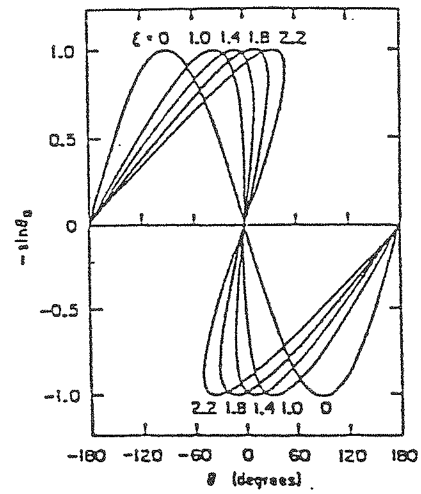

Figure 2 Constant ξ curves in phase space for a gap-and-drift prebuncher (from M. James)

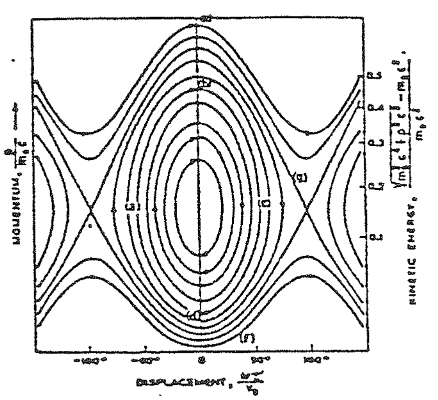

Figure 3 Constant phase velocity buncher phase space for $\beta_w < 1$ (from Slater)

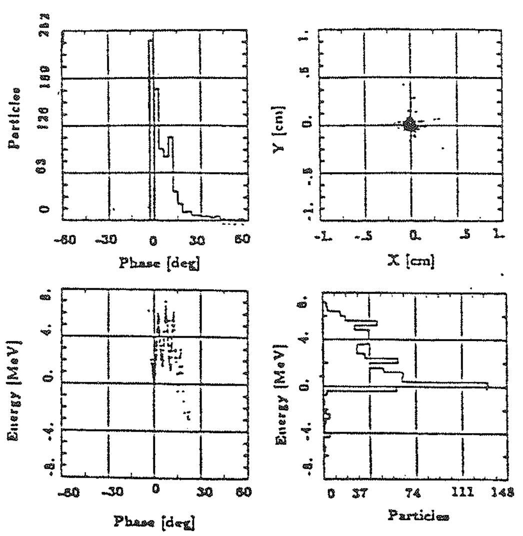

Figure 4 Beam simulation of electron bunch at the positron target

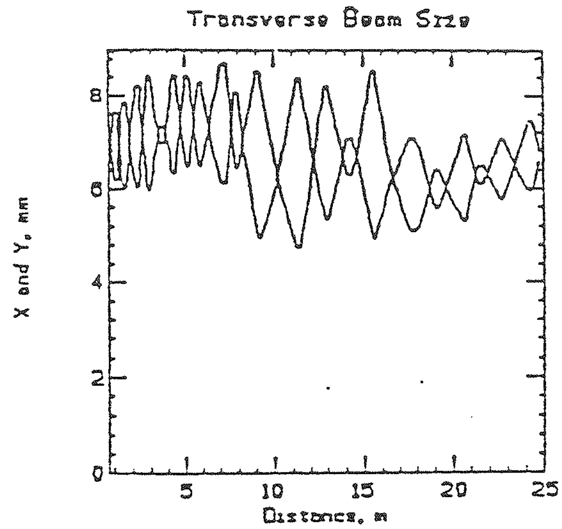

Figure 5 Beam envelope for positron accelerating sections

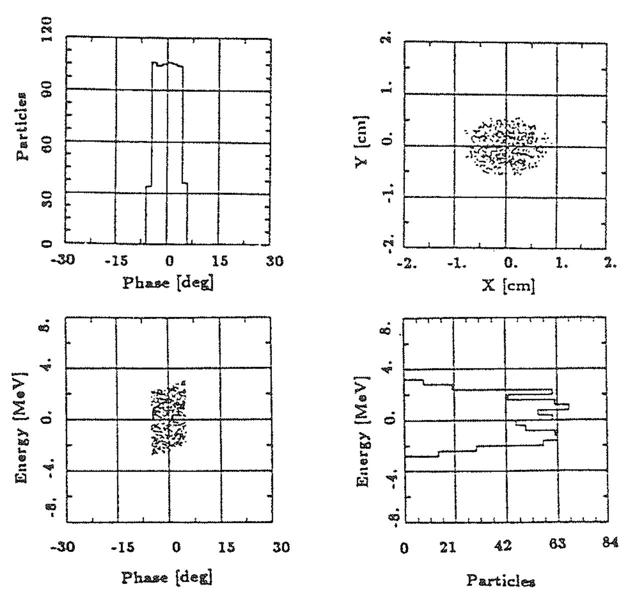

Figure 6 PARMELA simulation of positron beam at the end of the positron linac